JAAS

Journal of Analytical Atomic Spectrometry

www.rsc.org/jaas

Volume 25 | Number 3 | March 2010 | Pages 217–436

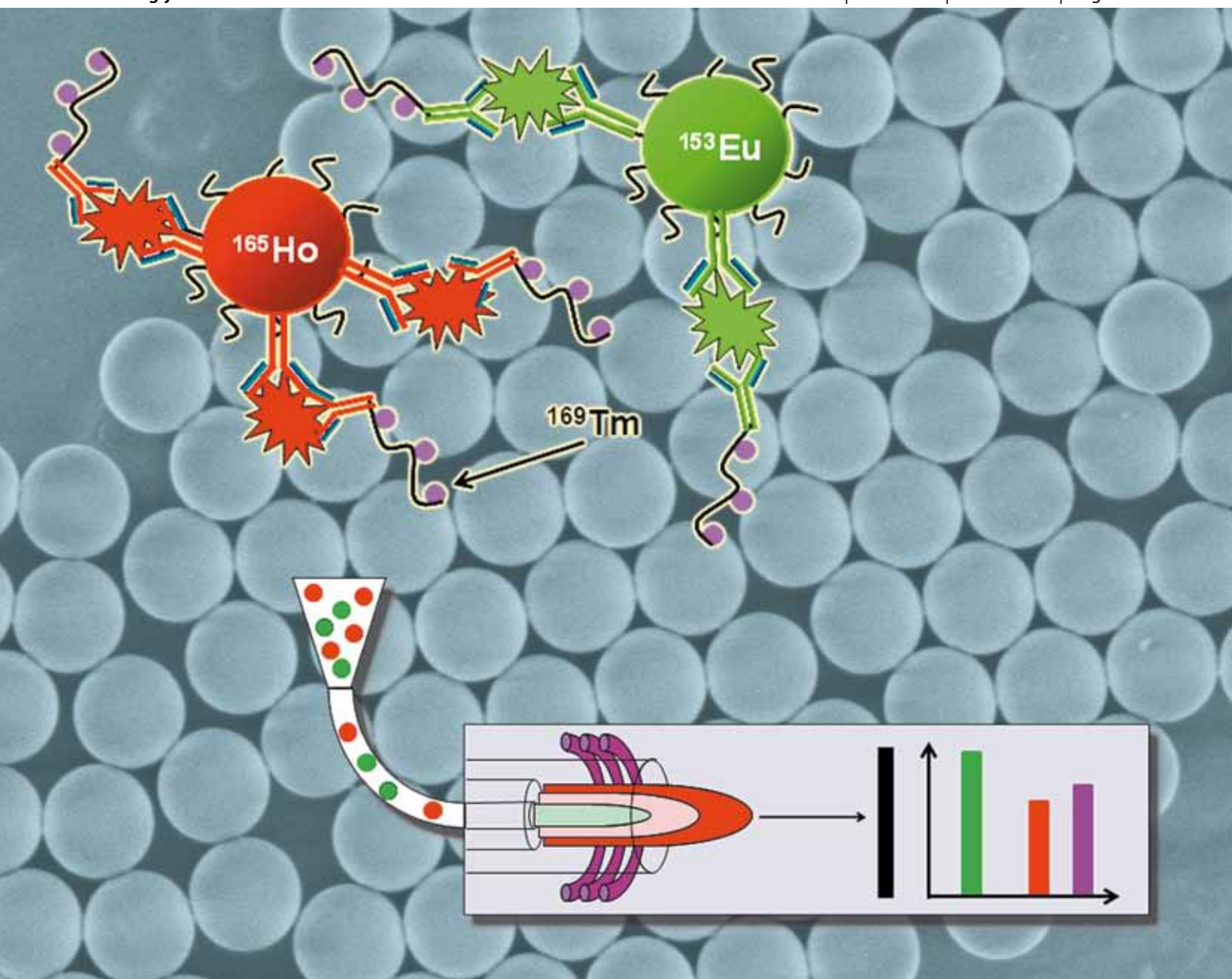

Themed Issue: Young Analytical Scientists

ISSN 0267-9477

RSC Publishing

Bio-functional, lanthanide-labeled polymer particles by seeded emulsion polymerization and their characterization by novel ICP-MS detection†‡

Stuart C. Thickett,§* Ahmed I. Abdelrahman, Olga Ornatsky, Dmitry Bandura, Vladimir Baranov* and Mitchell A. Winnik*

Received 18th August 2009, Accepted 8th December 2009
First published as an Advance Article on the web 24th December 2009
DOI: 10.1039/b916850h

We present the synthesis and characterization of monodisperse, sub-micron poly(styrene) (PS) particles loaded with up to and including 10^7 lanthanide (Ln) ions per particle. These particles have been synthesized by seeded emulsion polymerization with a mixture of monomer and a pre-formed Ln complex, and analyzed on a particle-by-particle basis by a unique inductively coupled plasma mass cytometer. Seed particles were prepared by surfactant-free emulsion polymerization (SFEP) to obtain large particle sizes in aqueous media. Extensive surface acid functionality was introduced using the acid-functional initiator ACVA, either during seed latex synthesis or in the second stage of polymerization. The loading of particles with three different Ln ions (Eu, Tb, and Ho) has proven to be close to 100% efficient on an individual and combined basis. Covalent attachment of metal-tagged peptides and proteins such as Neutravidin to the particle surface was shown to be successful and the number of bound species can be readily determined. We believe these particles can serve as precursors for multiplexed, bead-based bio-assays utilizing mass cytometric detection.

Introduction

A multiplexed assay is a process that allows for the simultaneous determination and quantification of a large number of analytes. Multiplexed assays are particularly important in biology and in medicine, because they allow one to determine a large amount of information with increased efficiency from small samples.[1–7] One class of multiplexed assays that is becoming increasingly prevalent are particle-based (often referred to as 'bead-based') assays where differing surface chemistries provide a route for detection and discrimination. These are similar to the use of microtiter plates, where various compositions and surface binding groups can be introduced to detect biological reagents. Particle-based assays have seen applications in immunological and gene expression assays.[8,9] Typically, particles are analyzed cytometrically, a method that has exhibited increased sensitivity and specificity over standard immunoassays.[10–13]

In cytometric detection, two markers are required. These are typically referred to as the 'classifier' marker (present within or on the surface of the particle) and the 'reporter' marker (attached to the reporter molecule, which may be an antibody, peptide or oligonucleotide). The most commonly used markers are fluorophores for luminescence detection,[3] such as for the well-known Luminex™ system.[14] The combination of the detection of both markers allows for the quantification of the analyte of interest. A family of different classifier markers that are detectable in the same analysis provides the ability to create a multiplexed assay.

We wish to develop a multiplexed, particle-based assay based on elemental (metal) tags for cytometric delivery followed by ICP-MS detection. To achieve this, our group has developed[15] an instrument that incorporates single particle delivery with mass spectrometric elemental detection. This instrument has been named a mass cytometer. The technical advantage of this approach is that the particles are introduced on an individual basis into the ICP ion source for analysis. The resolution and dynamic range of ICP-MS allows for the detection of a large number of elements (and their isotopes) simultaneously – far more than simultaneous detection based on fluorescence, which suffers from spectral overlap. Individual mass spectra in this instrument are collected continuously at high resolution of transient events which allows the determination of particle composition (*i.e.* type and concentration of the metal tag) in a precise manner. Members of the lanthanide (Ln) family were chosen to act as metal-based tags in this work, due to their similar chemistry, large number of resolvable isotopes and low natural abundance in biological/cellular systems.

To develop particle-based bio-assays using Ln tags for MS detection, particles containing a 'classifier' Ln tag must be synthesized, as well as molecules that can act as an Ln-based 'reporter' tag. In our group, we have demonstrated[16] that metal-chelating polymers (MCPs) synthesized by controlled-radical polymerization can chelate enough copies of a given Ln ion for ICP-MS analysis, as well as undergo covalent attachment to proteins and antibodies of interest, serving the purpose of a metal-based reporter tag. We are now turning our attention to

Chemistry Department, The University of Toronto, 80 St George Street, Toronto, ON, Canada M5S3H6. E-mail: sthicket@chem.utoronto.ca; mwinnik@chem.utoronto.ca; vladimir.baranov@utoronto.ca; Fax: +1 416 978 0541; Tel: +1 416 978 6495

† This article is part of a themed issue devoted to highlighting the work of outstanding young analytical scientists (YAS) working in the area of analytical atomic spectrometry. This 3rd YAS issue has been guest edited by Professor Spiros Pergantis.

‡ Electronic supplementary information (ESI) available: Experimental design, particle synthesis data, surface analysis, EDX linescan data, particle size distribution growth data, dynamic light scattering measurements and mass cytometric data. See DOI: 10.1039/b916850h

§ Current address: Schools of Chemistry and Chemical/Biomolecular Engineering, The University of Sydney, Sydney NSW 2006, Australia. Tel: +61 2 9351 7596

the development of polymer particles containing Ln ions to act as classifiers. The combination of Ln-tagged particles and polymeric Ln reporter tags, in conjunction with mass cytometric detection, forms the basis of our approach.

Polymer particles for the bio-assay applications outlined here must satisfy a number of important criteria. These are discussed in significant detail in the body of this paper, but briefly, they are as follows. The particles must be large (>500 nm) and monodisperse with respect to particle size – but not too large (>5 μm) to burn completely in the plasma torch. As we are measuring the composition of particles on an individual basis, the lanthanide content distribution (denoted LnCD) must also be narrow. The particles must also be loaded with a significant quantity of Ln (*e.g.* more than 10^6 ions per particle) for a high quality MS signal. Finally, the particles should have a surface that permits bioconjugation of proteins and oligonucleotides, with minimal non-specific adsorption.

A variety of possibilities exist for the synthesis of Ln-labeled polymer particles. Previously, it has been shown[17] that commercially available poly(styrene) (PS) particles with modified DTPA ligands were able to uptake Ln ions (specifically Gd^{3+}) for MRI enhancement purposes. In our own group, we have synthesized[18] PS and poly(methyl methacrylate) (PMMA) by miniemulsion polymerization where a hydrophobic Ln complex was pre-dissolved in the monomer prior to ultrasonication. As per the mechanisms of miniemulsion polymerization, however, these particles were of the order of 100 nm which is too small for our current applications. Recently, we have reported the synthesis of ~2 μm PS particles loaded with a variety of types and concentrations of different Ln ions by multiple-stage dispersion polymerization.[19] The synthesis of these particles has proven to be very successful and four different Ln ions (La, Tb, Tm and Ho) have been incorporated at five resolvable levels of concentration.

In this article, we present a new method for the synthesis of surface-functional, Ln-labeled polymer particles. We use a combination of surfactant-free emulsion polymerization (SFEP) to form monodisperse PS seed particles and then perform seeded emulsion polymerization with this system to grow these particles and load various Ln metals in the same step. The Ln loading step utilizes pre-formed, hydrophobic Ln complexes similar to those used in previous miniemulsion experiments. These complexes are soluble in monomers such as styrene. We use a mixture of styrene and complex to swell the seed particles prior to polymerization. The use of a well characterized, pre-formed seed and knowledge of the amount of Ln complex loaded allows for specific targeting of the Ln content per particle. Similarly, SFEP with functional initiators[20,21] allows for the creation of particles that can readily undergo bioconjugation through relevant surface chemistry. It is the combination of these properties, followed by novel mass cytometric analysis, that allows for the testing of these particles as potential candidates for bio-assay applications.

Experimental

Materials and reagents

Styrene (Sigma Aldrich, ReagentPlus, 98%) was washed with a 5% w/w KOH solution and subsequently passed through a column of basic alumina (150 mesh, 58 Å, Sigma Aldrich) prior to storage under refrigeration at 4 °C. Purified monomer was never kept for more than one week. Methyl-β-cyclodextrin (Me-β-CD, 50% w/w solution in water, a gift from Rohm and Haas Company) was used as received. Diethylenetriaminepentaacetic acid (>99%, DTPA, Sigma Aldrich) was used as received. Potassium persulfate (KPS, 99% ACS grade, Sigma Aldrich), sodium chloride (ACS grade, ACP Chemicals), sodium hydroxide (pellets, ACP Chemicals), sodium dodecyl sulfate (>99%, SDS, Sigma Aldrich), and sodium hydrogencarbonate (anhydrous, ACS grade, $NaHCO_3$, ACP Chemicals) were all used as received. 4,4′-azobis(4-cyanovaleric acid) (>98%, ACVA, Fluka) was used as received and stored at −18 °C. All water used was Milli-Q grade (Millipore). EDC ((1-ethyl-3-[3-dimethylaminopropyl]carbodiimide hydrochloride), Pierce Biotechnology), a zero-length crosslinker for coupling amines to carboxyl groups was used according to the manufacturers instructions. Sulfo-SMCC ((sulfosuccinimidyl 4-[*N*-maleimidomethyl]cyclohexane-1-carboxylate), Pierce Biotechnology) is a heterobifunctional crosslinker that contains an *N*-hydroxysuccinimide (NHS) ester and a maleimide group that allows covalent conjugation of amine- and sulfhydryl-containing molecules. NeutrAvidin™ Biotin-Binding Protein (Pierce Biotechnology), does not contain carbohydrate and has little tendency for non-specific protein binding. Reagents such as EDC, Sulfo-SMCC and Neutravidin were stored at −20 °C prior to use. BSA (bovine serum albumin V, Sigma) was used in blocking buffer (1% in phosphate buffer solution, PBS). Plain PS-COOH particles (P(S/V-COOH) 1.1 μm beads, Bangs Labs, #PC04N with carboxylic acid functionalization) were used as controls.

Surfactant-free emulsion polymerization (SFEP) using ACVA

A typical experiment is as follows. Water (85 g) was added to a three-necked round bottom flask equipped with a condenser, overhead stirrer (half-moon paddle) and gas inlet. To this, a certain amount of either NaCl or $NaHCO_3$ was added and allowed to dissolve. NaCl was added to mediate the total ionic strength of the aqueous phase to the desired level. $NaHCO_3$ also mediates the ionic strength while acting as a aqueous-phase buffer. Typically the amount added ranged from 0 to 0.225 g, and the total ionic strength (when including added base and initiator) varied from 20 to 50 mM. Styrene (10 g) was then charged into the flask and vigorous emulsification took place at 200 rpm for 30 min at room temperature under constant flow of nitrogen. The sample was then slowly raised to the reaction temperature (between 333 to 353 K) by means of a temperature-controlled oil bath.

In a separate flask, ACVA (0.055 g) was dissolved in basic water (0.02 g NaOH dissolved in 5 g water). Typically the ACVA concentration was between 2–2.5 mM. The amount of base was chosen to neutralize the two acid groups per initiator molecule and improve the water solubility of ACVA. When the reaction was at temperature, the initiator was introduced *via* syringe and polymerization was allowed to occur for 24 h. Final latex solids was checked by gravimetry; the latex was filtered through glass wool and stored until required for further analysis. Samples for seeded polymerization experiments were dialyzed for one week against daily changes of water (MW cut-off = 2000 Da dialysis membrane from SpectraPor).

Surfactant-free emulsion polymerization (SFEP) using persulfate

The synthesis of PS colloids using persulfate as initiator was performed in a manner analogous to the methods of Goodwin *et al.*[22,23] Using an identical polymerization reactor setup as previously described, water (75 g), NaCl (0.012 g), $NaHCO_3$ buffer (0.065 g) and styrene (9.9 g) were added to a polymerization vessel and vigorously emulsified for 30 min. The emulsion was deoxygenated using high-purity N_2. The vessel was raised to reaction temperature (333 K) and upon temperature stabilization, a solution of initiator (0.195 g KPS in 5 mL water) was injected by syringe. The total ionic strength of the aqueous phase was approximately 40 mM. Polymerization was allowed to take place for 24 h. The resultant latex was filtered through glass wool and dialyzed for one week. The latex made by this method used for further experiments was denoted st109.

Synthesis of lanthanide complexes

Hexadentate complexes of Eu(III), Tb(III) and Ho(III) were synthesized using 4,4,4-trifluoro-(1-napthyl)-1,3-butanedione (TNB) as the ligand according to literature procedures.[24] The complexes are denoted $Eu(TNB)_3$,$Tb(TNB)_3$ and $Ho(TNB)_3$ and their synthesis and characterization is reported in a previous article.[18]

Seeded emulsion polymerization

A typical protocol to load Ln complexes into the interior of either of the seed latexes used in this work is given here. Two methods are utilized in this work – the use of an acid-stabilized latex with KPS as the second stage initiator is denoted 'Method 1' while the use of a sulfate-stabilized latex with ACVA as the second stage initiator is denoted 'Method 2'.

Seed latex (corresponding to 0.1 g of polymer based on the solids content of the latex) was added to a small round bottom flask. To this, 1 mL of a 0.1% w/w solution of SDS (1 mg SDS total) in water was added and the flask shaken vigorously. SDS was added to provide additional colloidal stability as the particles grow. $NaHCO_3$ (0.018 g) was added to act as an aqueous phase buffer; additional water (7–13 g) was added to dilute the latex. The amount of water added was dependent on the solids content on the latex used; the aim was to finish with a latex that was of the same total solids content of the seed (assuming 100% conversion of the added monomer).

In a separate scintillation vial, one of the Ln complexes (or a mixture of complexes) was weighed out using an analytical microbalance (Mettler-Toledo). The mass of Ln complex dictates the theoretical target of the number of lanthanide ions per particle; for loadings of 10^6 Ln per particle, this typically corresponded to values around 2 mg of complex; loadings of 10^7 Ln per particle required on the order of 20 mg. This complex was then dissolved in styrene (0.4 g); given the size of the seed particles and planned temperature of reaction this amount was theoretically determined to be close to the saturation limit of 0.1 g of polymer particles. The specific amount, type and combination of Ln desired per particle were dependent on the choice and molecular weight of the complex used.

The monomer/complex mixture was then added to the latex solution and stirred magnetically in a sealed vessel overnight at room temperature. Methyl-β-cyclodextrin (Me-β-CD) was added to the emulsion prior to swelling. The amount of cyclodextrin added was dependent on the total amount (moles) of Ln complex being loaded into the particles; a five-fold molar excess of Me-β-CD (typically 0.05–0.3 g) was added relative to the complex. This long period of equilibration time was chosen to ensure effective swelling of the polymer particles. The following day, the sample was deoxygenated using high purity N_2, then raised to the reaction temperature (353 K). A separate initiator solution (either KPS or ACVA) was then injected *via* syringe (KPS: 0.03 g in 2 mL water, ACVA: 0.055 g in 3 mL of water with 0.019 g NaOH also present to ensure dissolution) and polymerization was allowed to take place for 24 h. After polymerization the sample was filtered through glass wool. A sample (2×2 mL) was centrifuged and redispersed into high purity water over four cycles to provide a clean sample for further analysis.

Surface acid titration

Surface acid titration analyses were performed in a method analogous to Kawaguchi *et al.*[25] Samples of latex were diluted in high-purity water to a solids content of 0.05% w/w. To this, 200 μL of a standardized 0.1 M NaOH solution was added by micropipette (Eppendorf) and stirred magnetically. This solution was then back-titrated using a 0.0098 M HCl solution (standardized separately against an 0.998 M solution of Na_2CO_3) added in volume increments ranging from 20 to 200 μL. Equivalence points corresponding to the titration of free base and the titration of deprotonated surface acid groups were monitored by both potentiometric and conductometric methods (using a Fisher Scientific conductivity meter and Ecomet pH probe). A blank solution (no latex) was titrated under the same conditions to account for dissolved carbon dioxide in the solution.

Lanthanide leaching experiments

An experiment was performed to test the stability of Ln-loaded seeded emulsion polymerization particles with respect to leaching of Ln into the aqueous phase. A seeded emulsion polymerization experiment (denoted ST141) was performed to synthesize particles loaded with $Eu(TNB)_3$ at a theoretical Eu loading of 1.06×10^7 per particle. Briefly, 'Method 2' (ACVA as second-stage initiator) was used to further grow latex st109 as described previously. The amounts of each reagent used were: 3.43 g st109 (corresponding to 0.1 g of seed polymer), 12.8 mg $Eu(TNB)_3$ dissolved in 0.403 g styrene, 0.024 g $NaHCO_3$, 1.03 mg SDS, 0.12 g Me-β-CD, 0.061 g ACVA, 0.02 g NaOH and 17 g total of additional water. A sample of the latex was cleaned by three centrifugation and redispersion cycles into water. The concentration of Eu in the (undiluted) latex by weight corresponded to 629 ppm.

To test leaching, a 1 mM solution of DTPA in water was prepared. The pH of the solution was 3.2. 1 mL of sample ST141 was then added to 10 mL of the DTPA solution; the amounts chosen were such that theoretically all of the encapsulated Eu could be chelated by the DTPA present. The solution was stirred magnetically at room temperature and 1 mL aliquots were taken at various time intervals. These aliquots were centrifuged for 5 min at 13 000 rpm and the supernatant of each was collected.

The supernatant of four samples were then analyzed by standard ICP-MS to measure the lanthanide content and determine the quantity of leaching. The supernatant was diluted by a factor of 10^3 for ICP-MS measurements.

Scanning electron microscopy (SEM) and energy-dispersive X-Ray spectroscopy (EDX)

Latex samples were prepared for scanning electron microscopy (SEM) by creating a 1 : 500 dilution of the latex sample in water and placing one drop of this solution on a Formvar/Carbon copper electron microscopy grid (Pelco, USA). Samples were analyzed in SE mode on the Hitachi S-5200 Scanning Electron Microscope (Centre for Nanostructure Imaging, The University of Toronto). The accelerating voltage was 1 kV and current 20 mA. For each sample, a series of images were taken; particle size distributions were constructed on the basis of counting at least 200 particles to provide meaningful statistics with regards to average size and polydispersity. Image analysis was performed using ImageJ.[26]

Using the energy-dispersive X-Ray spectroscopy (EDX) attachment (Inca, Oxford Instruments), composition-based linescans were performed on relevant particles detected on the sample grid. The accelerating voltage for EDX measurements was 20 kV and the current 20 mA. Data was collected for a period of ten minutes. The signal-to-noise ratio of the obtained signal was determined by considering the signal of an element known to not be present in the sample (*e.g.* Ti). EDX was used to determine incorporation of Ln ions into the particle interior.

Dynamic light scattering

Latex samples were diluted by a factor of approximately 5×10^{-5} in Milli-Q water. Right-angle dynamic light scattering (DLS) measurements were carried out at 25.00 ± 0.05 °C using an instrument from ALV described previously.[27] Size information was obtained by analysis of the autocorrelation function decay by CONTIN,[28] using software included with the ALV instrument.

Standard ICP-MS

Typical operating conditions of the ICP-MS instrument ELAN DRCPlus (Perkin-Elmer SCIEX) are based on a stable Ar plasma optimized to provide a <3% CeO^+/Ce^+ ratio in 1 ppb standard multielement solution diluted in 10% HCl. The requirement was achieved by applying 1400 W forward plasma power, 17 L/min Ar plasma gas flow, 1.2 L/min auxiliary Ar flow, and 0.95 L/min nebulizer (Burgener Micromist) Ar flow. Under these operating conditions, the typical sensitivity is 4×10^4 cps for 1 ppb Ir standard solution in 10% HCl. This instrument has single mass resolution for signal intensities in adjacent channels that do not differ by more than 10^6. The detection limits for lanthanide elements are less that 1 ppb. The sample uptake rate was adjusted depending on the particular experiment and sample size, typically 100 μL/min. A MicroFlow PFA-ST concentric nebulizer (Elemental Scientific, Inc) was used in all instances. Experiments were performed using an autosampler (Perkin-Elmer AS 91) modified for operation with Eppendorf 1.5 mL tubes. Sample size varied from 150 to 300 μL. Standards were prepared from 1000 μg/mL PE Pure Single-Element Standard solutions (Perkin-Elmer, Shelton, CT) by sequential dilution with high-purity deionized water (DIW) produced using an Elix/Gradient (Millipore, Bedford, MA) water purification system.

Bio-conjugation experiments

A typical bioconjugation procotol is as follows:

A sample of 10^9 polymer particles (the volume of which is dependent on N_p, however typically this was 10–20 μL) was washed twice by centrifugation in 50 mM MES, pH 5.2, 0.05% Proclin300 at 10000 g for 5 min. 170 μL of MES buffer was then added to the particles. A 0.2 g mL^{-1} solution of 1-ethyl-3-(3-dimethylaminopropyl)-carbodiimide (EDC) in MES buffer was prepared, and 20 μL of this solution was added to the particles and mixed with gentle vortexing. The sample was then split into two separate centrifuge tubes. 25 μL of Neutravidin (10 mg mL^{-1} solution) or 25 μL of a 10 mg mL^{-1} solution of BSA were added to separate tubes. Some samples were incubated with Neutravidin that was pre-labeled with a ^{169}Tm-labeled metal chelating polymer known as X4.[16] The tubes were mixed gently and allowed to react overnight at 4 °C. The particles were then pelleted at 5000 g for 20 min, and the blocking buffer 1% BSA in PBS was added. The beads were then sonicated for thirty minutes in a sonication bath. The supernatant was then aspirated.

For non-labeled Neutravidin samples, the introduction of a peptide 'reporter tag' for mass cytometry analysis then followed. For example, the CAB-Lu biotin-conjugated reporter tag, small peptide with a biotin molecule attached at one end and DTPA-Lu at the other end (Lu-DTPA-Asp-Leu-Leu-Val-Tyr-Asp-Lys(biotin)-amide, MW 1783.1 g/mol, synthesized at the University of Toronto) will bind to any Neutravidin conjugated to the particle surface. The beads were incubated with 100 μL of 500 nM of CAB-Lu in 1% BSA for 40 min at room temperature, then washed once with PBS and finally redispersed in a 0.26% w/w NaCl solution in 3 mM Tris buffer. The beads were then analyzed by mass cytometry. Another reporter tag used in this work included a pre-labeled IgG-Tm169, a mouse immunoglobulin with attached ^{169}Tm-X4.

Mass cytometer

The mass cytometer employed here is a new instrument recently introduced by DVS Sciences Inc. (Richmond Hill, Ontario, Canada) for the real time analysis of individual biological cells or microparticles. Cells or microparticles labeled with elemental tags (in this case, lanthanide ions) are introduced stochastically into the plasma torch of an inductively coupled plasma mass spectrometer with time-of-flight detection (ICP-TOF-MS). Since many available stable isotopes can be used as the tags, many proteins and gene transcripts can potentially be detected simultaneously in individual particles through the quantification of stable isotope tags bound to target biomarkers directly or indirectly using affinity molecules. The acquired data is saved in text and in FCS3.0 formats, the latter being compatible with third party flow cytometry data processing software, for example, FlowJo. A detailed description of the instrument can be found in Bandura *et al.*[29]

Results and discussion

Synthesis and characterization of monodisperse seed latexes

In this section, we report the synthesis and characterization of seed latexes (particles) for use in seeded emulsion experiments. To satisfy the requirements of a particle-based bio-assay based on mass cytometry analysis, the seed particles must have a narrow particle size distribution (PSD). A narrow PSD ensures that the distribution of Ln ions from particle to particle is as low as possible, which is crucial for subsequent multiplexed mass cytometry experiments. Also of importance is the presence of surface acid functionality for later bioconjugation. To achieve this, we synthesized PS seed latexes by surfactant-free emulsion polymerization (SFEP), using the acidic azo initiator ACVA in a method analagous to that presented by Bastos-Gonzalez *et al.*[20] SFEP is a very simple experimental process where hydrophobic monomers are polymerized under high shear in aqueous media in the absence of added surfactant. The SFEP process typically yields monodisperse and large (*i.e.* several hundred nanometres in diameter) polymer particles, and these particles are stabilized by the initiator end-groups that reside on the surface. The use of ACVA as the initiator for SFEP yields particles that have surface acid groups at the conclusion of polymerization.

In the work of Bastos-Gonzalez *et al.*[20] acid-stabilized particles were synthesized that were approximately 300 nm in diameter. This size is too small for our purposes, as the capacity for high Ln loading is reduced. Our aim was to obtain seed particles at least 500 nm in diameter. It is well known that the diameter of particles made by SFEP increases with increasing ionic strength of the aqeuous medium.[22,23] We chose conditions of high ionic strength in an attempt to synthesize larger particles stabilized by surface acid groups. High ionic strength conditions also aid in the synthesis of monodisperse colloids.

We were interested in investigating the experimental conditions that would allow us to synthesize PS latexes to meet the requirements discussed above. Experimental parameters that were varied included the polymerization temperature, ionic strength of the aqueous medium (through addition of NaCl) and the presence or absence of an aqueous-phase buffer ($NaHCO_3$). Experimental observables that were used to gauge the success of these syntheses were the average particle size and the breadth of the particle size distribution (PSD). An extensive description and data for all of the syntheses performed is presented in the Supplementary Information.‡ The reaction conditions that yielded latexes that were greater than 500 nm in diameter and with a particularly narrow PSD were conditions of high ionic strength (52 mM) in the absence of buffer, and a high polymerization temperature (353 K). The reproducibility of this synthesis is quite poor, and this is emphasized in the Supplementary Information.‡ An SEM image of the particles from this synthesis (sample st040) is shown in Fig. 1. From the PSD analysis of st040 we calculated a number-average diameter D_n of 528 nm and a coefficient of variation (CV_D) of 1.7%. This sample was ideal for our applications, and this sample was used as one of the seed latexes for further seeded growth experiments.

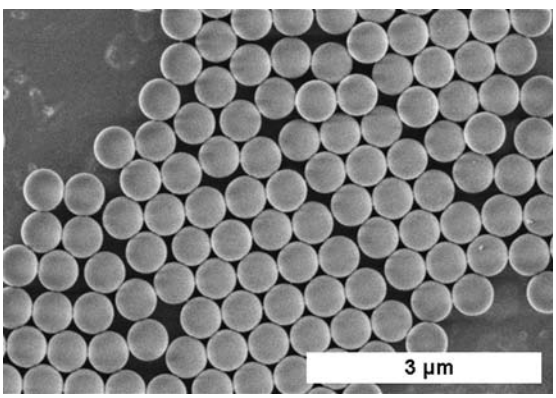

Fig. 1 SEM image of seed latex st040.

We observed that samples synthesized in the absence of buffer (such as st040) remained colloidally stable on the order of a few weeks after dialysis. We also synthesized PS particles with ACVA initiation in buffered media (addition of $NaHCO_3$ as opposed to NaCl). Large (>500 nm) particles could be synthesized at lower ionic strengths (approximately 25 mM). The shelf life of these was much greater after dialysis (on the order of months). SEM images of particles made using added buffer are provided in the Supplementary Information.‡ The sample made using aqueous-phase buffer used for further swelling experiments was denoted st153 ($D_n = 554$ nm, $CV_D = 1.6\%$).

In order to quantify the number of surface acid groups on particles synthesized with ACVA, we used surface acid titration experiments[25] (performed as a back titration). Titration curves (such as for the titration of st040) is presented in the Supplementary Information.‡ Two distinct equivalence points were observed, the first corresponding to the excess base and the second corresponding to protonation of the surface acid groups. The number of acid groups on the particle surface was calculated from the volume difference between the two equivalence points. On average, approximately 10^7 acid groups per particle were detected, with an error of approximately $\pm 10\%$.

The number of surface acid groups per particle after further growth of these particles was also determined by surface acid titration. A sample of seed latex st040 was swollen with a mixture of styrene and the lanthanide complex $Eu(TNB)_3$ and polymerized at 353 K with KPS as the initiator. This sample is denoted ST077 (sample codes that are capitalized represent seed particles that have been further polymerized by seeded growth). Averaging three separate measurements, the average number of acid groups (per particle) for sample ST077 was 0.87 ± 0.17 ($\times 10^7$). From this data we conclude that minimal loss of surface acid groups occurred after further growth.

There are two seeded growth protocols used in this work, and both are designed to introduce surface acid functionality at some stage during the synthesis. When an acid-functional seed latex (*i.e.* st040 or st153) was used, further polymerization was performed with potassium persulfate (KPS) as the initiator. This protocol was denoted 'Method 1.' We also used an alternative approach where ACVA was used as the initiator in the seeded emulsion polymerization step (known as 'Method 2' in this work), and the seed latex was prepared using KPS as the initiator. Using literature conditions,[23] a large monodisperse PS latex was synthesized by SFEP with persulfate initiation (denoted st109). The details of st109 are presented in Table 1 as well as in the Supplementary Information.‡ The use of both Methods is discussed in detail in the following section.

Table 1 Properties of latexes used as seeds in seeded emulsion polymerization experiments presented in this work

Sample	Surface groups	D_n (nm)	CV_D (%)	PDI	N_p (L^{-1})	Number of acid groups per particle
st040	Acid[a]	528	1.7	1.0009	2×10^{14}	1.33×10^7
st153	Acid[a]	555	1.6	1.0007	8.5×10^{14}	1.3×10^7
st109	Sulfate[b]	621	4.4	1.007	2.2×10^{14}	n/a

[a] Synthesized with ACVA as initiator. [b] Synthesized with KPS.

Particle growth results and comparison of methods

This section documents the results of seeded emulsion polymerization experiments to incorporate hydrophobic Ln complexes into the interior of polymer particles. We use the seed latexes described in the previous section and swell them with a solution of a hydrophobic Ln complex dissolved in monomer (styrene). Our experimental protocol was designed based upon established thermodynamics of particle swelling,[30] as we aimed to work under conditions where the particle interior was not saturated with monomer. The theoretical details of this experimental protocol are presented in the Supplementary Information.‡ This experimental protocol allowed us to target a specific Ln loading level (*i.e.* number of Ln ions per particle) based on the particle number density (N_p, units L^{-1}) and the mass of Ln complex added.

The first aim of these experiments was to observe the growth of seed particles in the presence of Ln complexes dissolved in monomer prior to swelling. To monitor this growth process, we measured the particle size distribution (PSD) after swelling and polymerization. We first performed a Method 1 polymerization (using seed latex st040) in an attempt to load 10^6 Eu ions per particle. SEM images (see Fig. 2A) of this sample showed significant amounts of secondary nucleation (new particle formation as opposed to growth of the seed particles). The extensive amount of secondary nucleation indicated that a significant fraction of the overall polymerization was occurring outside of the seed.

We hypothesized that the observed secondary nucleation was due to poor transport of the hydropobic Ln complex through the aqueous phase and into the particle interior. Methyl-β-cyclodextrin (Me-β-CD) is commonly used as a transport agent for hydrophobic materials in emulsion polymerization.[31,32] Thus we added Me-β-CD (in a molar excess relative to the added Ln complex) prior to swelling and subsequent polymerization to assist in the transport of the Ln complex through the aqueous phase. An SEM image of the product of this polymerization is given in Fig. 2B. Very few small particles were observed, and the seed-growth particles had grown in size and were still monodisperse. Calculated PSDs for these polymerizations are given in the Supplementary Information;‡ the reduction in the number of new particles formed is approximately a factor of 40. Due to the significant reduction in amount of observed secondary nucleation, all subsequent polymerizations were performed in the presence of Me-β-CD, regardless of the choice of initiator or polymerization method.

After establishing the benefits of addition of Me-β-CD as a transport agent, we next examined the reproducibility of the-seeded growth polymerization reaction. Particle growth

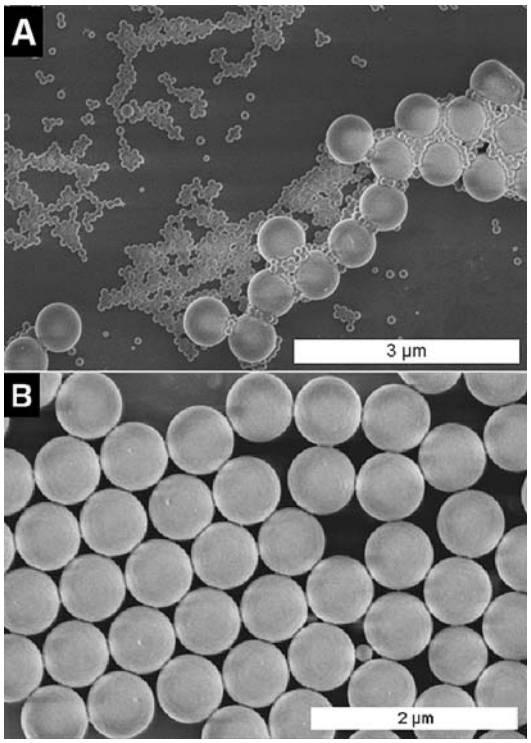

Fig. 2 SEM image analysis of the seeded growth of st040 by Method 1 polymerization (KPS as initiator) for the attempted loading of Eu at 10^6 ions per particle. Shown are (A) – polymerization in the absence of Me-β-CD and (B) – polymerization in the presence of Me-β-CD.

consistency was evaluated on the basis of the amount of observed secondary nucleation. For each synthesis, the *number* PSD was determined by sizing and counting particles in SEM images using the ImageJ software package,[26] with particle diameter step sizes of 10 nm. An example of a typical number PSD is shown in Fig. 3. Distributions were grouped into the seeded growth particles and the 'new' particles (smaller particles formed in the seeded growth step). The entire number PSD was normalized and the *volume* PSD calculated. From the PSD, the volume fraction of the distribution that was due to new particles was determined (denoted Φ_{NEW}). A low value of Φ_{NEW} indicates little secondary nucleation in the particle growth step.

Fig. 4 shows Φ_{NEW} values for polymerizations using Method 1 (st040 seed, KPS initiation) as well as Method 2 (st109 seed, ACVA initiation). Most Φ_{NEW} values were between 1–5%. The data show that small levels of secondary nucleation occur during the particle growth step for both Method 1 and Method 2. The amount of secondary nucleation, however, varies between samples. This result is problematic with respect to optimizing experimental reproducibility, but it does not interfere with the use of these particles for applications and for mass cytometry analyses. The population of small particles can be readily removed from each sample by centrifugation and redispersion of the sample into water.

For potential bio-assay applications, the final PSD after seeded growth should be narrow. A narrow PSD has the effect of reducing the variation in lanthanide content from particle to particle, which is critical for mass cytometry analysis. In order to evaluate the breadth of the PSD, the coefficient of variation

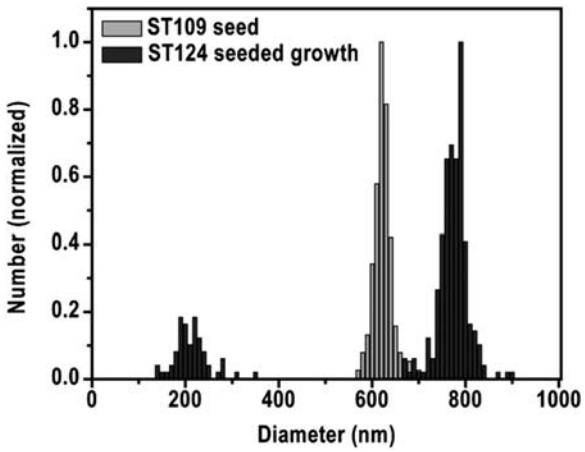

Fig. 3 Number PSD of sample ST124 (seeded emulsion polymerization of st109 *via* Method 2 to load Eu at a target of 1.17×10^7 ions per particle. Shown in the PSD histogram is the original seed PSD (light grey) as well as the PSD after seeded growth (dark grey) prior to further centrifugation and washing. Note the population due to secondary nucleation at approximately 200 nm diameter. These are washed away during centrifugation.

(CV_D) of the particle population after growth was determined by numerical analysis of the number PSD for each sample. Fig. 3 presents the final PSD (dark grey) of sample ST124 (Method 2 polymerization of st109 at a theoretical Eu loading of 1.17×10^7 ions per particle). The seed PSD is shown in light grey. From Fig. 3, we see that the diameter of the seed particles increased from 620 nm to approximately 800 nm, and a small population of smaller particles was formed. The distribution of the larger particles is narrow ($CV_D = 4.7\%$). This CV_D value is close to the tabulated value for the st109 seed (see Table 1).

Replicate experiments were performed to test the reproducibility of the seeded particle growth process. Four experiments were performed using Method 1 polymerization (acid-stabilized seed, KPS initiation) and six with Method 2 (sulfate-stabilized seed, ACVA initiation). The results (final number-average diameter and CV_D) of these experiments are presented in Table 2. The average value of CV_D from this data is $4.8 \pm 2.2\%$, but there is considerable scatter in the final particle diameter. We would ultimately like a greater consistency in the final particle size for later applications of these particles.

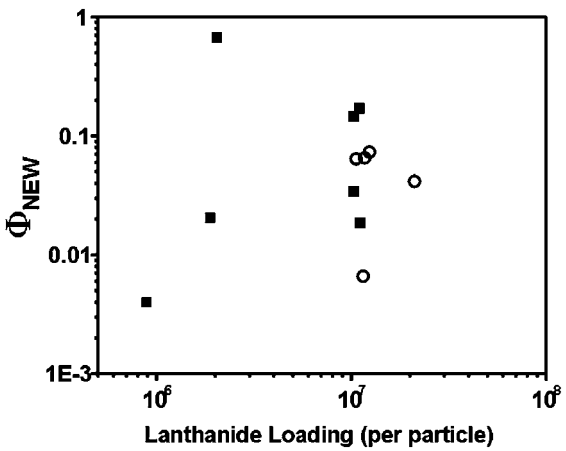

Fig. 4 Amount of secondary nucleation (expressed as Φ_{NEW}, the volume fraction of new particles from the volume PSD for each sample) plotted as a function of theoretical Ln loading per particle. Shown are seeded emulsion polymerization systems initiated by persulfate (black squares, 'Method 1') and by ACVA (open circles, 'Method 2').

Table 2 Variation in particle diameter and amount of secondary nucleation as a function of seeded emulsion polymerization method and replication of experiment

Sample	Method[a]	D_n (nm)	CV_D (%)
ST073	1	633	4.3
ST077	1	650	2.9
ST162	1	821	5.3
ST167	1	744	2.4
ST120	2	699	7.5
ST124	2	771	4.7
ST125	2	726	5.7
ST130	2	854	2.6
ST141	2	759	3.4
ST154[b]	2	714	9.2

[a] Experiments performed with quantity of seed latex corresponding to 0.1 g polymer. Other reagents: 0.4 g styrene, 0.25 g Me-β-CD, 15 mg $NaHCO_3$, 1 mg SDS, 15–20 mg of $Ln(TNB)_3$ complex, 10 g additional water. [initiator] = 10 mM. Polymerization for 24 h at 353 K after 24 h of swelling. [b] ST154 performed with 10-fold reduction in initiator (ACVA) concentration.

EDX Spectroscopy was used to examine Ln loading in the particle interior. Over a series of particles at a number of different sites on the microscopy grid, elemental linescans were used to characterize the particle composition. Typical profiles are shown in the Supplementary Information.‡ The linescans indicate uniform distribution (on the basis of profile shape) of the Eu^{III} throughout the particle core. There was no evidence that the Eu^{III} was localized near the particle surface or detected outside of the particles. This result served as a pre-cursor to the extensive quantitative analysis of the particles by mass cytometry, which is discussed in the next section.

Particle analysis by mass cytometry

We used mass cytometry, a unique instrument developed in our laboratories,[15,29] to provide quantitative determination of the Ln content of our particles on an individual basis. A cartoon of the instrument is depicted in Scheme 1; further details of the instrument are provided in Ref. 27. Briefly, the metal-labeled particles are introduced (*via* cytometric delivery and nebulization from dilute solution) into the ICP torch on an individual basis, and the atomic composition of the particles is determined by TOF-MS. Mass spectra are collected on the order of 10–20 μs, and as the ion cloud corresponding to each particle passes through the TOF chamber, multiple spectra are collected for each particle. TOF-MS data demonstrating the transit of Eu-labeled particles through the mass cytometer is presented in Supplementary Information.‡ The compilation of these spectra allows for the metal signature of particles to be determined and distributions created on the basis of metal content. For the analysis of our particles, both the *average* Ln content per particle can be determined, as well as the Ln content *distribution* (denoted LnCD). Comparisons between the theoretical and experimentally determined Ln loading values can be made.

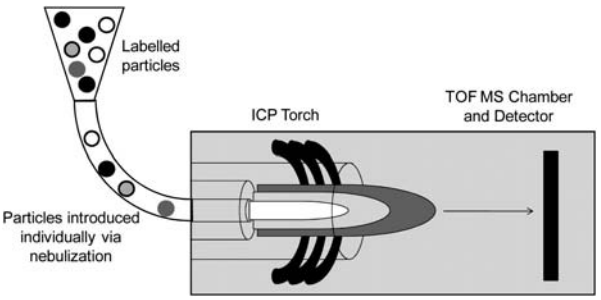

Scheme 1 Cartoon schematic of the mass cytometer instrument. Metal-labeled particles are introduced into the ICP torch on an individual basis, whereby they are burned and the atomic composition of each particle is determined by TOF-MS. Mass spectra are recorded on the order of every 20 μs. The size of the ion cloud corresponding to each particle as it passes through the TOF chamber allows for 20 to 30 mass spectra to be collected per particle.

For multiparameter bio-assay applications, the LnCD should be narrow (*i.e.* small CV_{Ln}). In this case, one will be able to synthesize particles loaded with a given Ln ion at different concentration levels. We examine the breadth of the LnCD of the particles described here in terms of their measured mass cytometry response. The majority of the particle samples synthesized in this work were loaded with Eu. Eu has two isotopes (^{151}Eu and ^{153}Eu) with significant and approximately equal abundance. Because of this, isotopic 'dot-plot' diagrams can be created that reveal the spread of Eu loading from particle to particle. An Eu dot-plot from sample ST162 (targeted loading of 1.03×10^7 Eu per particle, approximately 5×10^6 of each isotope) is presented in Fig. 5. It should be noted that the actual *number* of Eu ions per particle is equivalent to the Eu *intensity* (on the axes of Fig. 5) multiplied by an ion transmission/detection efficiency of 2300. (The instrument ion transmission/detection efficiency relates the number of ions generated in the plasma torch to the number of ions detected by the TOF data acquisition system, and is specific for each element. Further information on mass cytometry calibration is given in Abdelrahman *et al.*[33]) The colour of the dots in this diagram reflect the mangitude of the number of particles detected with that specific Eu loading, with blue the lowest and red the highest. On both isotopic axes, there are particle events that range in intensity values from 10^3 to over 10^5, meaning that some particle events have 100 times more Eu than others. A long blue tail appears in the data in Fig. 5, stretching to high Eu intensity values. One interpretation of these results is that the LnCD is not very narrow.

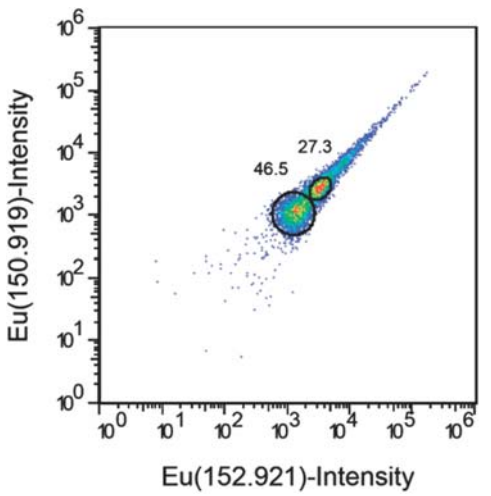

Fig. 5 Eu isotopic dot-dot diagram for sample ST162 (particles loaded with Eu with targeted value of 1.03×10^7 per particle) as measured by mass cytometry. Two main peaks (circled) and a long tail are evident.

Closer inspection of Fig. 5 reveals two intense red spots (circled) in the data, that represent two dominant particle populations detected by mass cytometry. The numbers in Fig. 5 represent the percentage of the total particle population represented by the two respective peaks. For this specific example, the mean intensity for ^{153}Eu (the choice of isotope is arbitrary) in the first peak is 1400 counts, while for the second peak the mean intensity is 3100 counts. The ratio of the mean intensity of these two peaks in this sample is ~2.3. Given the breadth of these distributions, we consider the second peak to be the 'doublet' of the first peak. This conculsion is supported by the fact that both Eu isotopes show the same relative increase in intensity. Additional isotopic diagrams and LnCDs are provided in Supplementary Information,‡ and all samples (except one) demonstrate, to varying extents, the appearance of 'doublet' and 'higher order' peaks. The most likely cause of this effect is particle aggregation and the resulting detection and analysis of 2 (or more) particles at the same time.This hypothesis is supported by dynamic light scattering (DLS) measurements of these particles in solution. The measured autocorrelation function for sample ST162 (and other samples after seeded growth) suggests some particle aggregation in solution. These results are presented in the Supplementary Information.

From isotopic dot-plots such as the one shown in Fig. 5, we can calculate one-dimensional LnCDs by projecting the data along one of the chosen axes (depending on the isotope we wish to consider). Fig. 6 presents a histogram of the data in Fig. 5 for ^{153}Eu to create two LnCDs for this particular isotope. In Fig. 6, the two peaks represent the two circled populations in Fig. 5; the higher intensity peak is the 'doublet' of the lower intensity (solid line) peak, emphasizing the multimodal nature of the distribution. We calculated the coefficient of variation (CV_{Ln}) of only the first population, using the data processing capabilities in the FlowJo software package. The values of CV_{Ln} obtained from this first peak were used as a measure to describe the quality of Ln loading in the second stage of the polymerization process.

The coefficients of variation (CV_{Ln}) of the first peak in all experimentally determined LnCDs are provided in the Supplementary Information.‡ CV_{Ln} values are typically greater than 20%, and sometimes as high as 40%. The values of CV_{Ln} and the breadth of the LnCD can then be compared to the breadth of the PSD of each sample. The value of CV_D for the final PSDs of the latexes after seeded growth are of the order of ~4%, which translates to a variation in the particle *volume* of slightly more than 10%. The variation in the distribution of the lanthanide is consistently greater than this, suggesting non-uniform partitioning on the basis of particle volume.

We calculated the average Ln per particle from the experimentally obtained LnCD. It is worth emphasizing that as the obtained LnCDs contain two (or more) peaks, the average number of Ln ions per particle was calculated from the statistics

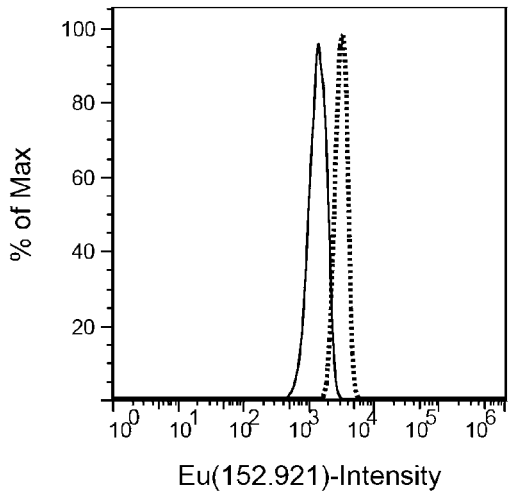

Fig. 6 Lanthanide content distribution (LnCD) for ^{153}Eu from sample ST162 (obtained from Fig. 5). The two peaks shown here correspond to the two populations observed by mass cytometry. Note than the number of ions per particle is related to intensity by a factor of 2300.

of the first peak in isolation. This was assumed to be valid as additional peaks were considered to be due to simultaneous detection of two or more particles The average number of Ln ions per particle is related to the calculated average *intensity* from CyTOF data multiplied by a particular ion transmission/detection efficiency *coefficient* (an instrument constant) whose values were determined by calibration of the instrument. For more details, see Bandura *et al.*[29]

We compared the experimentally determined average Ln per particle with the theoretically predicted value from the experimental design. This comparison is presented in Fig. 7. Data in Fig. 7 is provided for Method 1 and Method 2 seeded emulsion polymerizations. The theoretical (dark grey) and experimental (pale grey) average Ln loadings (per particle) shown in Fig. 7 are in excellent agreement with one another. This agreement between experiment and theory was achieved for the three complexes tested ($Eu(TNB)_3$, $Tb(TNB)_3$ and $Ho(TNB)_3$). Sample ST130 was prepared with a mixture of $Eu(TNB)_3$ and $Tb(TNB)_3$. The data in Fig. 7B shows that both Eu and Tb were detected at values near their predicted amounts in this synthesis. CV_{Ln} values for the two metals in this experiment (Eu = 26%, Tb = 21%) were similar to CV_{Ln} values obtained in experiments where only one metal was loaded into the particle interior. The CV_{Ln} values for all analyzed samples are reported in the Supplementary Information.‡

The data in Fig. 7 suggests that the Ln loading process is reproducible and consistent between experimental analyses. The first five results reported in Fig. 7B represent five separate syntheses in which $Eu(TNB)_3$ was loaded into seed latex st109. In all five cases, the experimentally determined average Ln per particle is close to the predicted value, and the results are consistent from sample to sample. It is somewhat surprising that we find such consistency in Ln loading despite the variation in final particle size of these samples (see Table 2), ranging from 699 nm to 854 nm (a variation of close to 20%). We infer from this result that the lanthanide transport is efficient and is not affected by secondary nucleation (which only affects the final particle size).

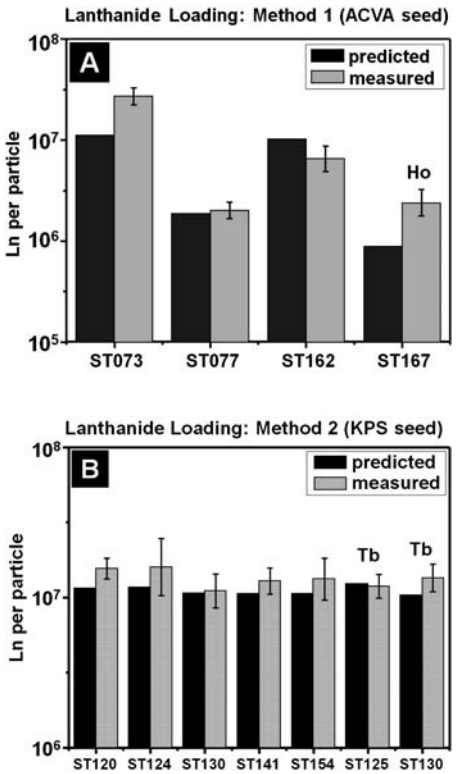

Fig. 7 Lanthanide loading *via* seeded emulsion polymerization: comparison of theoretically predicted loading values with experimentally determined averages from mass cytometry. (A): Ln loading using 'Method 1.' (B): Ln loading using 'Method 2.' The dark colours correspond to the predicted value for each sample. Unless otherwise indicated, the Ln complex used is $Eu(TNB)_3$. Experimental average Ln values are obtained from the first peak in each LnCD from mass cytometry.

Finally, the data suggest that both polymerization methods result in efficient Ln loading. There is no obvious trend to suggest that one method (*i.e.* choice of seed latex and second stage initiator) gives consistently higher or lower Ln loading results. Both methods are useful for the synthesis of Ln-labeled particles by seeded emulsion polymerization The caveat remains the nature and breadth of the measured LnCD, but we can conclude that the seeded emulsion polymerization method allows access to very high, quantitative loading concentrations.

We believe that the loading of multiple metals in one seeded emulsion polymerization reaction should be possible. Multiple metals, loaded at a variety of different concentrations, provide the ability to significantly expand the number of uniquely resolvable particles for bio-assay purposes. These experiments, and testing the resolvability of different Ln concentration levels by mass cytometry, is the subject of ongoing work within our group.

Stability of particles towards Ln leaching

In this section, we examine the stability of particles with respect to Ln leaching. To be candidates for bio-assay applications, the particles must satisfy two criteria; there must be no leaching of Ln ions when stored in aqueous media, as well as under conditions of bioconjugation. We used conventional ICP-MS analysis of the supernatant (after centrifugation of the sample) to

determine the aqueous-phase Ln concentration. Three sets of conditions were chosen to monitor Ln leaching – particles dispersed in pure water, particles dispersed in a pH 5.2 buffer to mimic bioconjugation conditions and particles dispersed in the presence of a strong metal chelating agent (DTPA) dissolved in the aqueous phase.

The first analysis was that of the supernatant of a purified sample of ST077. Sample ST077 contains an average of 2×10^6 Eu per particle. ST077 was purified by centrifugation and redispersion into pure water three times at pH 7. The total Eu content of this sample was 260 ppm. The supernatant was analyzed after three months' storage, and the Eu content of the supernatant (measured by ICP-MS) was 60 ppb. This aqueous-phase concentration is the equivalent of the leaching of 0.02% of the total content of loaded lanthanide.

In a separate experiment, a sample of Ln-labeled particles was dispersed in the presence of a Ln chelating agent (1mM DTPA, pH 3.2). The aim of this experiment was to monitor the Ln concentration in the supernatant as a function of time. Ln leaching was evaluated in this experiment using a sample of latex ST141 with an Eu content of 1.3×10^7 ions per particle. Aliquots were taken from a 1 : 10 diluted latex sample over different periods of time (ranging from thirty minutes to one week) and the supernatant of the centrifuged latex was analyzed by ICP-MS. Detected Eu concentrations were very low (2.6–2.8 ppb), and the concentration remained approximately constant over time. This result suggests that after an initial release, no further leaching of Eu from the particle interior takes place. The amount of Eu lost represents approximately 5% of the total metal content. This amount is much greater than that found for storage of an equivalent sample in water at neutral pH, but still not deleterious to the use of these particles for bioassays.

A final study of the stability of these particles with respect to Ln leaching was performed under conditions that replicated those used in bioconjugation experiments (*i.e.* in dispersed media at pH 5.2). A sample of latex ST141 was dispersed in an acetic acid/sodium acetate buffer adjusted to pH 5.2, and aliquots were taken from this solution over time in an identical manner to the procedure discussed above. The aliquots were centrifuged and the supernatant analyzed by ICP-MS. In this experiment, the detected Eu concentrations were extremely low (2–3 parts per trillion) and there was no variation in this Eu concentration over time. These Eu concentrations are the equivalent of the loss of 0.05% of the total metal content into the aqueous phase. This amount is so small that it can be considered insignificant and we can infer that the particles do not leach lanthanide under conditions used in bioconjugation experiments.

The combination of the results presented in this section indicate that the Ln-tagged particles synthesized by this method are stable with respect to Ln leaching under a range of different conditions. No leaching of metals from the particle interior takes place after prolonged storage in neutral aqueous media, while only minimal Ln loss occurs at acidic pH in the presence of a strong metal chelating agent. The particles are also stable under conditions used for surface functionalization. As a result, we conclude that these particles are stable with respect to utilization as part of bio-assay applications, with the added advantage of a long shelf life.

Bioconjugation and potential use for bio-assay applications

In this section, we discuss the ability of proteins and antibodies to be covalently attached to the particle surface. The general procedure used for the conjugation of proteins to the surface of Ln-tagged particles is as follows. A metal-chelating copolymer (MCP) with a thiol end-group and approximately 30 metal-chelating sites (pendant DTPA groups) along the backbone (synthesized by controlled-radical (RAFT) polymerization). This polymer was covalently attached to Neutravidin (a deglycosylated version of avidin) using the coupling agent sulfo-SMCC (sulfosuccinimidyl 4-[*N*-maleimidomethyl]cyclohexane-1-carboxylate). Sulfo-SMCC reacts with amine groups on Neutravidin (through the presence of an *N*-hydroxysuccinimide group) and, *via* the present maleimide functionality, with the thiol group on the MCP. The linked MCP was loaded with ^{169}Tm ions to create a metal-tagged protein. EDC (1-ethyl-3-[3-dimethylaminopropyl]carbodiimide hydrochloride) was then used to activate surface carboxylic acid groups on the particle; incubation of these particles with the metal-tagged Neutravidin led to covalent coupling through an amine residue.

To test the availability of the surface –COOH groups for biofunctionalization of the particles synthesized here, we carried out a parallel comparison of ST073 with commercial PS particles that have a carboxylated surface (1.1 micron diameter PC04N PS particles, Bangs Labs). ST073 has a Eu content of 2.7×10^7 per particle, whereas there are no Ln ions in the core of the commercial particles. Both particles were tested for labeling with Neutravidin. These particle-Neutravidin conjugates were analyzed by mass cytometry. The experimentally determined Ln content distributions (LnCDs) for Eu and Tm are shown in Fig. 8. We used a 40-fold molar excess of sulfo-SMCC with respect to the MCP for the coupling reaction, followed by attachment of the tagged Neutravidin to the particles. The results from this preparation are show in as a solid line in Fig. 8. Finally, the measured LnCDs from the commercially available particles are shown using a dashed line.

The Tm distributions for this analysis are presented in Fig. 8A. The data in the solid line is comparable in Tm intensity to the data for bioconjugation to the commercial particles (dashed line). The mean Tm intensity of the solid line is 4.5×10^3. When this mean intensity is converted to the number of Tm per particle, we calculate a mean value of approximately 2.5×10^6. We assume each MCP carries approximately 30 copies of the Tm ion. If there are, for example, 8 MCPs covalently attached to each Neutravidin, then we can estimate that there are approximately 10^4 Neutravidins bound to each particle.

Fig. 8B presents the Eu content distribution. The commercial particles (dashed line) contain no Eu and this is reflected in the distribution at low intensity values determined by mass cytometry. The low intensity values (10–100 counts) spanned by this distribution are the equivalent of 'background' values by mass cytometry. The dashed line distribution appears broad simply due to the presentation of the data on a logarithmic scale. The Eu distribution from sample ST073 (solid line) has a very high mean intensity. Data for bioconjugation to other particles, such as those synthesized by 'Method 2' (ACVA as the second stage initiator) is given in the Supplementary Information.‡ The conclusion we can draw from these experiments is that particles

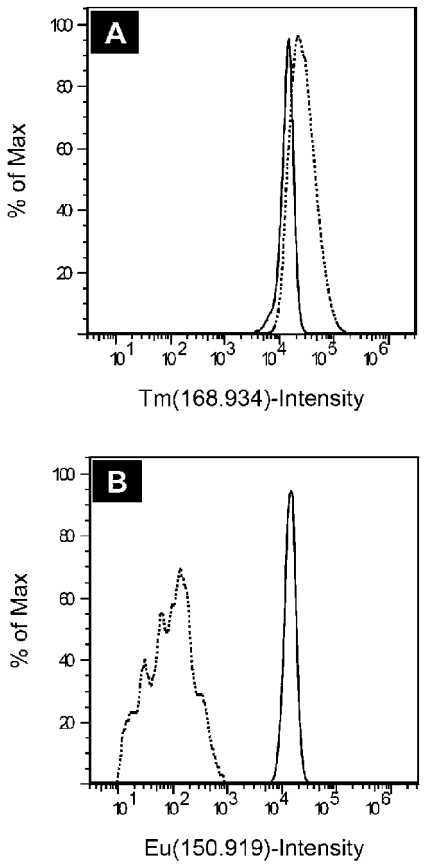

Fig. 8 LnCDs for A) ^{169}Tm and B) ^{151}Eu for the conjugation of labeled Neutravidin to acid-stabilized particles ST073. Key: Dashed line **---** commercially available PS-COOH particles; Solid line **—** ST073 labeled with Neutravidin with reduced X4 with 40 fold excess of SMCC.

made by our synthetic methods are comparable to commercially available particles with respect to bioconjugation.

The next set of model bioconjugation experiments were designed to detect three metals simultaneously. These experiments involved prototype sandwich assays based on mass cytometry detection. As presented in Scheme 2, we exposed particle-Neutravidin conjugates (again from sample ST073) to biotin-labelled mouse IgG. Biotin has an extremely strong affinity for avidin. We incubated these conjugates with goat anti-mouse-IgG that was prelabeled with a MCP carrying copies of ^{159}Tb.[16] The entire system was then analyzed by mass cytometry. In principle, we should be able to simultaneously detect the metal in the particle core (Eu), on the Neutravidin (Tm) and on the antibody (Tb).

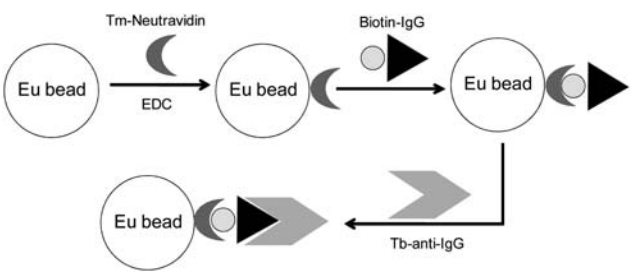

Scheme 2 Schematic of particle metal-labeled sandwich immunoassay for mass cytometry analysis.

We present the experimentally determined LnCDs for the three metals in this system in Fig. 9. These distributions correspond to the same preparative conditions discussed above and presented in Fig. 8. We only consider the data in these three distributions from a qualitative standpoint, however accurate determination of the number of copies of each ion attached to the Neutravidin and the anti-IgG would allow for quantification of the numbers of these groups per particle.

We consider the LnCDs shown in Fig. 9. The Eu signal (Fig. 9A) originates from the metal label in the particle core. The Eu distribution is broad and multimodal. The Tm signal (Fig. 9B) originates from the labeled Neutravidin. The Tb signal

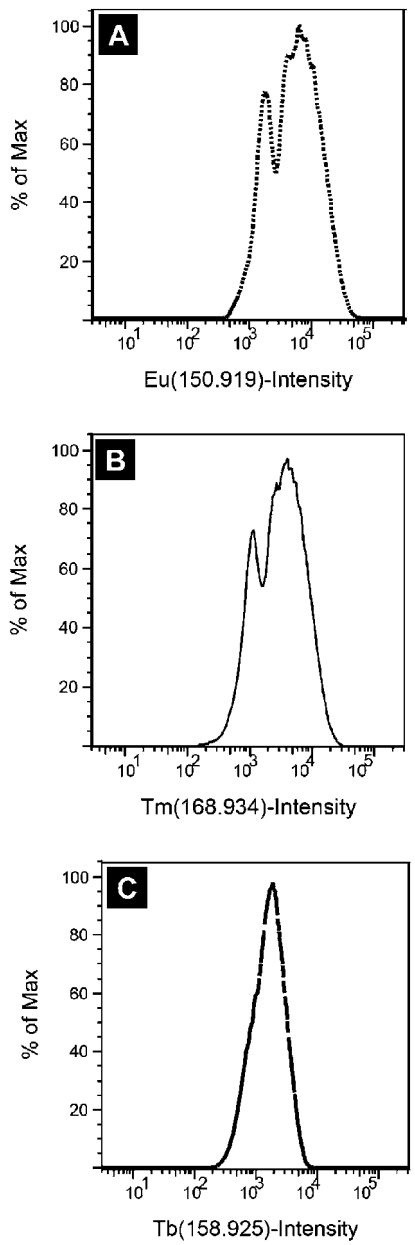

Fig. 9 Mass cytometry analysis used for a model sandwich assay involving ST073 particles labeled with Tm-tagged Neutravidin, treated with biotin-labeled mouse IgG, in turn recognized with Tb-tagged anti-mouse IgG. The LnCD of the all three detected elements are shown.

(Fig. 9C) is from the labeled goat anti-mouse-IgG. All three metals are readily detectable as part of the same analysis.

Conclusions

In this work, we described the synthesis and characterization of surface-functional, lanthanide-labeled polystyrene particles. These particles were designed to have applications in bio-assays that involve multiplexed detection of biological moieties.

The method chosen to synthesize these particles was a combination of surfactant-free emulsion polymerization (SFEP) and seeded emulsion polymerization utilizing a dissolved, hydrophobic lanthanide (Ln) complex. SFEP provided many technical advantages for this work – large particle sizes, monodisperse particle size distributions and the presence of an extensive number of surface acid groups per particle when the acid-functional azo initiator ACVA was used. The number of acid groups per particle was approximately 10^7 as determined by surface acid titration.

The use of seeded emulsion polymerization, with mixtures of styrene and Ln complexes as the swelling medium and methyl-β-cyclodextrin as a transport agent, provided the ability to target the desired Ln loading level per particle. All experiments were designed to load over 10^6 Ln per particle, with the most typical target being 10^7 – a very high loading concentration for particles of sub-micron dimensions. Small (<5% of the total polymer volume) amounts of secondary nucleation were formed in the second stage of these syntheses, but could be easily removed by centrifugation and redispersion of the larger particles.

The Ln content per particle was determined by mass cytometry analysis. The instrumental design allows for introduction of individual particles and their analysis by ICP-MS detection. Ln signals were measured for particles loaded with individual Ln ions – Eu, Tb and Ho, as well as with mixtures of Ln complexes. The lanthanide content distributions (LnCDs) of these particles, however, were quite broad (CV $\sim$ 20%) and multiple populations were detected in most analyses. This result was attributed to weak particle agglomeration in the instrument or during sample preparation, and learning to prevent this aggregation is an ongoing topic of research in our group.

The average Ln content per particle by mass cytometry was in excellent agreement with the theoretically predicted loading value. The procedure was reproducible for a range of metals at a range of different Ln loading concentrations. The particles were shown to be stable with respect to storage in aqueous media and no leaching occured under conditions required for bio-conjugation.

The usefulness of these particles for bead-based bioassays was tested in two model experiments. Neutravidin (pre-labeled with a Tm-containing metal chelating polymer) was attached to the surface of the Eu-labelled particles using EDC chemistry, and mass cytometry analysis demonstrated extensive surface binding through simultaneous measurement of both metal tags. These particles with surface-bound Neutravidin were then exposed to biotin-labelled IgG followed by goat anti-mouse-IgG (pre-labeled with a Tb-containing metal chelating polymer). All three metal tags were readily detected by mass cytometry in this experiment.

While there are still problems to be overcome, the results presented in this paper demonstrate that particle-based bioassays using polymer particles made by a combination of SFEP and seeded emulsion polymerization are possible. Similarly, the use of metal-based tags for detection by ICP-MS as an alternative to existing (fluorophore-based) technologies is achievable with particle analysis by the novel mass cytometer instrument. Given the ability to resolve so many metal tags at the same time, we see this as an exciting tool for high-throughput diagnostic analysis in the future.

Acknowledgements

The authors thank NIH (grant R01-076127) and NSERC Canada for their support of this research. Mr Jieshu Qian is greatly thanked for dynamic light scattering measurements. This study was conducted with the support of the Ontario Institute for Cancer Research (OICR) through funding provided by the Government of Ontario.

Notes and references

1 S. Brenner, M. Johnson, J. Bridgham, G. Golda, D. H. Lloyd, D. Johnson, S. Luo, S. McCurdy, M. Foy, M. Ewan, R. Roth, D. George, S. Eletr, G. Albrecht, E. Vermaas, S. R. Williams, K. Moon, T. Burcham, M. Pallas, R. B. DuBridge, J. Kirchner, K. Fearon, J.-I. Mao and K. Corcoran, *Nat. Biotechnol.*, 2000, **18**, 630–634.
2 E. B. Cook, J. L. Stahl, L. Lowe, R. Chen, E. Morgan, J. Wilson, R. Varro, A. Chan, F. M. Graziano and N. P. Barney, *J. Immunol. Methods*, 2001, **254**, 109–118.
3 S. A. Dunbar, C. A. Vander Zee, K. G. Oliver, K. L. Karem and J. W. Jacobson, *J. Microbiol. Methods*, 2003, **53**, 245–252.
4 E. R. Goldman, A. R. Clapp, G. P. Anderson, H. T. Uyeda, J. M. Mauro, I. L. Medintz and H. Mattoussi, *Anal. Chem.*, 2004, **76**, 684–688.
5 M. Han, X. Gao, J. Z. Su and S. Nie, *Nat. Biotechnol.*, 2001, **19**, 631–635.
6 P. Hardenbol, F. Yu, J. Belmont, J. MacKenzie, C. Bruckner, T. Brundage, A. Boudreau, S. Chow, J. Eberle, A. Erbilgin, M. Falkowski, R. Fitzgerald, S. Ghose, O. Iartchouk, M. Jain, G. Karlin-Neumann, X. Lu, X. Miao, B. Moore, M. Moorhead, E. Namsaraev, S. Pasternak, E. Prakash, K. Tran, Z. Wang, H. B. Jones, R. W. Davis, T. D. Willis and R. A. Gibbs, *Genome Res.*, 2005, **15**, 269–275.
7 J. P. Nolan and L. A. Sklar, *Trends Biotechnol.*, 2002, **20**, 9–12.
8 J. R. Epstein, J. A. Ferguson, K.-H. Lee and D. R. Walt, *J. Am. Chem. Soc.*, 2003, **125**, 13753–13759.
9 R. C. Bailey, G. A. Kwong, C. G. Radu, O. N. Witte and J. R. Heath, *J. Am. Chem. Soc.*, 2007, **129**, 1959–1967.
10 H. Harma, T. Soukka and T. Lovgren, *Clin. Chem.*, 2001, **47**, 561–568.
11 E. Morgan, R. Varro, H. Sepulveda, J. A. Ember, J. Apgar, J. Wilson, L. Lowe, R. Chen, L. Shivraj, A. Agadir, R. Campos, D. Ernst and A. Gaur, *Clin. Immunol.*, 2004, **110**, 252–266.
12 K. Na, S. Kim, K. Park, K. Kim, D. G. Woo, I. C. Kwon, H.-M. Chung and K.-H. Park, *J. Am. Chem. Soc.*, 2007, **129**, 5788–5789.
13 J.-M. Nam, C. S. Thaxton and C. A. Mirkin, *Science*, 2003, **301**, 1884–1886.
14 L. Yang, D. K. Tran and X. Wang, *Genome Res.*, 2001, **11**, 1888–1898.
15 S. D. Tanner, D. R. Bandura, O. Ornatsky, V. I. Baranov, M. Nitz and M. A. Winnik, *Pure Appl. Chem.*, 2008, **80**, 2627–2641.
16 X. Lou, G. Zhang, I. Herrera, R. Kinach, O. Ornatsky, V. I. Baranov, M. Nitz and M. A. Winnik, *Angew. Chem.*, 2007, **119**, 1–5.
17 I. Paschkunova-Martic, C. Kremser, K. Mistlberger, N. Shcherbakova, H. Dietrich, H. Talasz, Y. Zou, B. Hugl, M. Galanski, E. Sölder, K. Pfaller, I. Höliner, W. Buchberger, B. Keppler and P. Debbage, *Histochem. Cell Biol.*, 2005, **123**, 283–301.
18 C. Vancaeyzeele, O. Ornatsky, V. I. Baranov, L. Shen, A. Abdelrahman and M. A. Winnik, *J. Am. Chem. Soc.*, 2007, **129**, 13653–13660.
19 A. I. Abdelrahman, S. Dai, S. C. Thickett, O. Ornatsky, D. Bandura, V. I. Baranov and M. A. Winnik, *J. Am. Chem. Soc.*, 2009, **131**, 15276–15283.

20 D. Bastos-Gonzalez, J. L. Ortega-Vinuesa, F. J. De Las Nieves and R. Hidalgo-Alvarez, *J. Colloid Interface Sci.*, 1995, **176**, 232–239.
21 J. L. Ortega-Vinuesa, D. Bastos-Gonzalez and R. Hidalgo-Alvarez, *J. Colloid Interface Sci.*, 1995, **176**, 240–247.
22 A. R. Goodall, M. C. Wilkinson and J. Hearn, *J. Polym. Sci., Polym. Chem. Ed.*, 1977, **15**, 2193–2218.
23 J. W. Goodwin, J. Hearn, C. C. Ho and R. H. Ottewill, *Colloid Polym. Sci.*, 1974, **252**, 464–471.
24 L. R. Melby, N. J. Rose, E. Abramson and J. C. Caris, *J. Am. Chem. Soc.*, 1964, **86**, 5117–5125.
25 S. Kawaguchi, A. Yekta and M. A. Winnik, *J. Colloid Interface Sci.*, 1995, **176**, 362–369.
26 W. S. Rasband, National Institutes of Health, Bethesda, Maryland, 1997–2008, p. http://rsb.info.nih.gov/ij/.
27 G. Guerin, J. Raez, I. Manners and M. A. Winnik, *Macromolecules*, 2005, **38**, 7819–7827.
28 S. W. Provencher, *Comput. Phys. Commun.*, 1982, **27**, 213–227.
29 D. R. Bandura, V. I. Baranov, O. I. Ornatsky, A. Antonov, R. Kinach, X. Lou, S. Pavlov, S. Vorobiev, J. E. Dick and S. D. Tanner, *Anal. Chem.*, 2009, **81**, 6813–6822.
30 M. Morton, S. Kaizerman and M. W. Altier, *J. Colloid Sci.*, 1954, **9**, 300–312.
31 Y. Liu, J. C. Haley, K. Deng, W. Lau and M. A. Winnik, *Macromolecules*, 2008, **41**, 4220–4225.
32 C. C. Rusa, C. Luca and A. E. Tonelli, *Macromolecules*, 2001, **34**, 1318–1322.
33 A. I. Abdelrahman, O. Ornatsky, D. Bandura, V. I. Baranov, R. Kinach, S. Dai, S. C. Thickett, S. D. Tanner and M. A. Winnik, *J. Anal. At. Spectrom.*, DOI: 10.1039/b921770c.